

Article

Remediation of Methyl Orange Dye in Aqueous Solutions by Green Microalgae (*Bracteacoccus* sp.): Optimization, Isotherm, Kinetic, and Thermodynamic Studies

Ahmad Al Shra'ah ^{1,*}, Abdullah T. Al-Fawwaz ² , Mohammed M. Ibrahim ¹  and Eid Alsbou ³

¹ Department of Chemistry, Faculty of Science, Al al-Bayt University, P.O. Box 130040, Al-Mafraq 25113, Jordan; mohammadibrahim@aabu.edu.jo

² Department of Biological Sciences, Al al-Bayt University, P.O. Box 130040, Al-Mafraq 25113, Jordan; al_fawwaz@aabu.edu.jo

³ Department of Chemistry, Al-Hussein Bin Talal University, Ma'an P.O. Box 71111, Jordan; ealsbou@ahu.edu.jo

* Correspondence: aalshraah@aabu.edu.jo; Tel.: +962-777288033

Abstract: This study aims to assess the ability of old, immobilized fresh, and free fresh green microalgae (a *Bracteacoccus* sp.) to remove methyl orange (MO) dye from aqueous solutions. The effects of four factors, including initial MO concentration (5–25 mg L⁻¹), adsorbent dose (0.02–0.10 g mL⁻¹), temperature (4–36 °C), and contact time (5–95 min), were examined. The Box–Behnken design (BBD) was used to determine the number of required experiments and the optimal conditions expected to provide the highest removal percentage of MO dye from aqueous solutions. The experimental data were applied to four isotherm models (Langmuir, Freundlich, Dubinin–Radushkevich (D–R), and Temkin isotherm models) and three kinetic models (pseudo–first–order, pseudo–second–order, and Elovich kinetic models). The results indicate that the highest removal of MO (97%) could be obtained in optimal conditions consisting of an initial MO concentration of 10.0 mg L⁻¹, an adsorbent dose of 0.10 g mL⁻¹, a temperature of 20 °C, and a contact time of 75 min. Moreover, the experimental data were best fitted by the Langmuir and Temkin isotherm models and followed a pseudo-second-order kinetic model. The interaction between MO and the *Bracteacoccus* sp. was confirmed by UV and ESI/MS analyses, indicating that MO removal occurred via both sorption and degradation processes.

Keywords: methyl orange; algae; removal; Box–Behnken design; kinetics; isotherm



Citation: Al Shra'ah, A.; Al-Fawwaz, A.T.; Ibrahim, M.M.; Alsbou, E. Remediation of Methyl Orange Dye in Aqueous Solutions by Green Microalgae (*Bracteacoccus* sp.): Optimization, Isotherm, Kinetic, and Thermodynamic Studies. *Separations* **2024**, *11*, 170. <https://doi.org/10.3390/separations11060170>

Academic Editor: Xiaoying Guo

Received: 8 May 2024

Revised: 21 May 2024

Accepted: 28 May 2024

Published: 30 May 2024



Copyright: © 2024 by the authors. Licensee MDPI, Basel, Switzerland. This article is an open access article distributed under the terms and conditions of the Creative Commons Attribution (CC BY) license (<https://creativecommons.org/licenses/by/4.0/>).

1. Introduction

Industrial activities are significantly increasing, resulting in the discharge of massive amounts of effluent into the environment. This leads to water pollution, a critical issue that requires significant attention [1]. Many industries, such as textile, cosmetic, leather, paper, plastic, printing, rubber, and pharmaceutical industries, produce effluents containing synthetic dyes [2]. These synthetic dyes are classified into ionic (cationic and anionic) and nonionic (vat and disperse) dyes. In terms of toxicity, ionic dyes are more toxic because they are more reactive and carcinogenic [3]. Methyl orange (MO) dye is an example of ionic dye and is widely used in the textile industry and in research laboratories as an indicator in acid–base titrations [4]. MO dye can cause skin allergies, death (in the case of exposure to a high MO concentration), vomiting, and diarrhea [5]. Therefore, the uptake of synthetic dyes from contaminated water is a necessary step to protect the aquatic environment from pollution. Several techniques, such as membrane filtration, coagulation–flocculation, ozonation, photocatalytic oxidation, electrochemical oxidation, and adsorption, have been used to remove synthetic dyes from aqueous media [6]. Among these techniques, adsorption is considered the most appropriate for its several advantages, such as simplicity, low cost, environmental friendliness, effectiveness, and ease of use [7].

In general, the adsorbents used for adsorption of MO dye from aqueous solutions include biosorbents, activated carbon, biochar, minerals and clays, resins and polymers,

nanoparticles, and composites [8]. Among them, biosorbents are preferred for being easily available, environmentally friendly (they do not form intermediate products), highly efficient, regeneratable, and low-cost. Based on biosorbent sources, biosorbents can be classified into (i) natural biosorbents (e.g., straw, peels, chitosan, zeolites, etc.); (ii) microbial biomass (e.g., algae, bacteria, yeasts, and fungi); (iii) agricultural and industrial wastes (e.g., wheat bran, sawdust, etc.) [9]. Using algae in bioremediation has been described as an attractive and promising method because algae grow quickly and are highly effective in removing pollutants from aquatic systems. [10]. In previous studies, algal biosorbents such as *Fucus vesiculosus* [11], *Oedogonium subplagiostomum*-AP1 [12], *Chlorella* species, and algal blooms [13] were used to remove MO from aqueous solutions with reasonable removal efficiency (>50%). However, the optimization of MO removal to obtain a high removal efficiency at room temperature within a short time, the confirmation of MO removal/degradation, and the study the effect of immobilization of a biosorbent on the efficiency of MO removal from aqueous solutions require further investigation. In the literature, there are few studies related to the use of green microalgae for the treatment of wastewater polluted by dyes. Therefore, the current study adds new results regarding MO removal using green microalgae (a *Bracteacoccus* sp.) as a green method for the treatment of wastewater containing synthetic dyes.

In fact, adsorptive removal mainly depends on factors such as initial adsorbate concentration, adsorbent dose, temperature, and contact time [14]. Therefore, the optimization of these experimental variables is an essential step that can be achieved by the traditional experimental method (i.e., studying the effect of each factor while keeping the other factors constant), but the main drawbacks of this strategy are ignoring the interactions between the variables and needing a larger number of experiments as the number of variables increases. Consequently, an alternative experimental strategy is using response surface methodology (RSM) as a statistical and mathematical tool to design the experiments. RSM takes into account the interactions between the experimental variables and easily determines the optimum conditions that can provide the best response [15]. RSM can use a full or fractional factorial design, a central composite design (CCD), a Box–Behnken design (BBD), and a Doehlert matrix design (DMD) [16]. Amongst them, the BBD is favored for achieving better results [17]; therefore, it was used in the current study.

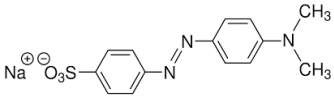
The main objectives of the current study were (i) to evaluate the ability of the *Bracteacoccus* sp. (old, fresh, and immobilized) to remove MO dye from aqueous solution; (ii) to optimize the experimental variables, including initial MO concentration, adsorbent dose, temperature, and contact time using the BBD; (iii) to describe the equilibrium and the adsorption kinetics of MO removal by a *Bracteacoccus* sp.; (iv) to investigate the reusability of the *Bracteacoccus* sp. for MO removal from aqueous solutions.

2. Materials and Methods

2.1. Materials

All chemicals used in the current study were of analytical grade and were used without further purification. MO dye (Table 1) was selected as a model anionic dye and purchased from Sigma Aldrich. A stock solution of MO dye (1000 mg L^{-1}) was prepared by dissolving a precise amount (1.000 g) of MO dye in 1000 mL of distilled water and was then used to prepare a set of MO diluted solutions with concentrations in the range of $5\text{--}25 \text{ mg L}^{-1}$. A calibration curve using the MO solutions in the concentration range of $5\text{--}25 \text{ mg L}^{-1}$ was established.

Table 1. Characteristics of MO dye [18].

Parameter	Value
Chemical structure	
Chemical formula	C ₁₄ H ₁₄ N ₃ SO ₃ Na
Molecular weight (g mol ⁻¹)	327.33
Molecular size (Å)	15.8 × 6.5 × 2.6
λ _{max} (nm)	464
Density at 20 °C	1.28
pKa	3.42
Solubility (mg L ⁻¹)	5.0 × 10 ³

2.2. Sampling of Green Microalgae

Green microalgae samples were collected from ground water in the west part of Mafrqa city in Jordan and directly transferred to the laboratory. Subsequently, green microalgae cultivation was carried out in flasks containing Bold Basal Medium (BBM). Furthermore, the isolation of algal colonies was conducted by establishing a series of subcultures in BBM agar plates. A pure culture was prepared from algal colonies and then examined microscopically. Routine cultivation was conducted at 25 ± 2 °C under a light intensity of $20.25 \mu\text{Em}^{-2}\text{s}^{-1}$ for 25 days. A pure culture was chosen and was identified as consisting of a *Bracteacoccus* sp.

2.3. Immobilization of the *Bracteacoccus* sp.

The immobilization of the *Bracteacoccus* sp. was accomplished based on the procedure described in a previous study [19]. In detail, a solution of sodium alginate (3%) was well mixed with a suspension of the *Bracteacoccus* sp. in a 2:1 ratio (*v/v*). The mixture was then transferred dropwise into a calcium chloride (CaCl₂) solution (0.03 M) to form adsorbent beads, remaining for 30 min into the CaCl₂ solution to become more solid. Thereafter, the beads were washed three times with distilled water and stored in the fridge at 4 °C for later use.

2.4. Characterization of the MO Solutions

The analysis of the MO dye solutions before and after adding the *Bracteacoccus* sp. was accomplished using (i) a UV Vis diode-array spectrophotometer (Specord S 600-Molecular Spectroscopy, Germany) operated in the wavelength range of 210–790 nm, with a quartz cuvette; (ii) a high-resolution TOF-MS/MS system (impact II Bruker, Bruker Daltonik, Bremen, Germany) and an impact II ESI-Q-TOF system equipped with a Bruker Daltonik Elute UPLC system (Bremen, Germany), as shown in Supplementary Materials.

2.5. Adsorption Experiments

The experiments of MO adsorption from an aqueous solution using the free fresh *Bracteacoccus* sp. were conducted in batch mode. The effect of several experimental factors, such as initial MO concentration, adsorbent dose, temperature, and contact time, on MO removal from aqueous solutions was investigated. In detail, 20.0 mL of MO solution (5–25 mg L⁻¹) was transferred to a 50.0 mL test tube, and then a desired adsorbent dose (0.02–0.10 g mL⁻¹) was added at a specific temperature in the range of 4–36 °C. The mixture was kept in a dark place on the lab bench for a desired time (5–95 min), and then a small portion (~2.0 mL) of the mixture was withdrawn, and its absorbance was measured at 464 nm. All the experiments were conducted in triplicate. The initial pH of the MO solutions was 4, which was described as the optimum pH value for acquiring the highest removal % of MO from aqueous solutions [11].

Subsequently, the removal efficiency percentage ($R\%$) of MO dye and the adsorption capacity (q_m), which represents the amount of dye that can be absorbed by 1.0 g of adsorbent (mg g^{-1}), was calculated using Equations (1) and (2), respectively [20].

$$R\% = \frac{C_o - C_t}{C_o} \times 100\% \tag{1}$$

$$q_m = \frac{(C_o - C_t)V}{m} \tag{2}$$

where C_o (mg L^{-1}) is the initial concentration of the MO dye solution, C_t (mg L^{-1}) is the concentration of the MO dye solution at time t , V (L) is the volume of the MO dye solution, and m (g) is the adsorbent amount used.

Design Expert version 8 was used to determine the required experiments, and a BBD based on RSM with a quadratic model was used. These experiments allowed for studying the effects of four experimental variables, namely, initial MO concentration (A), adsorbent dose (B), temperature (C), and contact time (D), each set at three levels ($-1, 0, +1$), as summarized in Table 2. Consequently, the overall required experiments were 29, as shown in Table 3, and the number of experiments (N) was determined using the following equation (Equation (3)) [21]:

$$N = 2K(K - 1) + M_o \tag{3}$$

where K and M_o are the number of experimental variables and the center points, respectively.

Table 2. Four experimental factors and their levels and actual values using a Box-Behnken design for MO dye removal using green microalgae (a *Bracteacoccus* sp.).

Parameter	Factor	Level		
		Low (-1)	Medium (0)	High ($+1$)
Initial MO concentration (mg L^{-1})	A	5	15	25
Adsorbent dose (g mL^{-1})	B	0.02	0.06	0.10
Temperature ($^{\circ}\text{C}$)	C	4	20	36
Contact time (min)	D	5	45	95

Table 3. BBD matrix for the four examined experimental factors (initial MO concentration, adsorbent dose, temperature, and contact time) including their coded values.

Exp. #	Factor 1 (Initial Concentration, mg L^{-1})	Factor 2 (Adsorbent Dose, g mL^{-1})	Factor 3 (Temperature, $^{\circ}\text{C}$)	Factor 4 (Time, min)
1	0	-1	-1	0
2	-1	0	0	-1
3	0	-1	0	-1
4	$+1$	0	-1	0
5	0	0	0	0
6	$+1$	0	0	-1
7	0	$+1$	0	$+1$
8	$+1$	0	$+1$	0
9	0	0	-1	-1
10	0	0	-1	$+1$
11	-1	-1	0	0
12	0	$+1$	0	-1
13	0	0	0	0
14	-1	0	0	$+1$
15	-1	$+1$	0	0
16	0	-1	$+1$	0
17	$+1$	-1	0	0
18	-1	0	$+1$	0

Table 3. Cont.

Exp. #	Factor 1 (Initial Concentration, mg L ⁻¹)	Factor 2 (Adsorbent Dose, g mL ⁻¹)	Factor 3 (Temperature, °C)	Factor 4 (Time, min)
19	0	0	0	0
20	+1	+1	0	0
21	0	0	0	0
22	-1	0	-1	0
23	0	0	+1	-1
24	0	+1	+1	0
25	+1	0	0	+1
26	0	0	+1	+1
27	0	+1	-1	0
28	0	-1	0	+1
29	0	0	0	0

2.6. Isotherm Study

Four common isotherm models, namely, Langmuir [22] (Equation (4)), Freundlich [23] (Equation (6)), Dubinin–Radushkevich (D-R) [24] (Equation (7)), and Temkin [25] (Equation (10)), were applied to the experimental data.

$$\frac{C_e}{q_e} = \frac{1}{K_L q_e^{max}} + \frac{C_e}{q_e^{max}} \tag{4}$$

$$R_L = \frac{1}{1 + K_L C_o} \tag{5}$$

where q_e (mg g⁻¹) is the MO amount adsorbed at equilibrium, q_e^{max} is the maximum adsorption capacity (mg g⁻¹), K_L (L mg⁻¹) is the Langmuir constant related to the adsorbent–adsorbate affinity and associated with sorption energy, and R_L , expressed in Equation (5), is a dimensionless equilibrium constant used to describe the adsorption process as irreversible ($R_L = 0$), linear ($R_L = 1$), favorable ($0 < R_L < 1$), or unfavorable ($R_L > 1$). The parameters q_e^{max} and K_L are calculated by plotting a linear relationship between C_e/q_e and C_e to obtain a slope of $1/q_e^{max}$ and an intercept of $1/(K_L q_e^{max})$.

$$\log q_e = \log K_f + \frac{1}{n} \log C_e \tag{6}$$

where K_f ((mg g⁻¹)(L mg⁻¹)^{1/n}) is the Freundlich isotherm constant, and n represents the heterogeneity factor (i.e., the non-linearity degree between the concentration of the dye solution and the absorption process), with the adsorption process being favorable when $n > 1$ [26]. By plotting a linear relationship between $\log C_e$ and $\log q_e$, the n and K_f values are calculated from the slope and intercept, respectively.

$$\ln q_e = \ln q_m + K_D \varepsilon^2 \tag{7}$$

$$E = \frac{1}{\sqrt{2K_D}} \tag{8}$$

$$\varepsilon = RT \ln \left(1 + \frac{1}{C_e} \right) \tag{9}$$

where K_D is the absorption energy constant (mol²/kJ²) used to calculate the average of sorption free energy E (KJ mol⁻¹) provided by Equation (8), with adsorption being physical ($E < 8$ KJ mol⁻¹), based on ion exchange ($E = 8–16$ KJ mol⁻¹), or chemisorption ($E = 20–40$ KJ mol⁻¹) [27]. In Equation (9), ε is the Polanyi potential (KJ mol⁻¹), R is the

universal gas constant (8.314×10^{-3} KJ mol⁻¹), and T is the temperature (K). By plotting a linear relationship between $\ln q_e$ and ε^2 , the slope (K) and intercept ($\ln q_m$) are obtained.

$$q_e = \frac{RT}{b_T} \ln A_T + \frac{RT}{b_T} \ln C_e \tag{10}$$

$$B_T = \frac{RT}{b_T} \tag{11}$$

where b_T is the Temkin constant and refers to the sorption heat (J mol⁻¹), and A_T is the Temkin isotherm constant (L g⁻¹). The A_T , B_T , and b_T values can be calculated by plotting a linear relationship between q_e and $\ln C_e$ to obtain the slope (B_T) and the intercept ($B_T \ln A_T$).

2.7. Kinetic Study

The experimental data were analyzed using three common kinetic models, namely, the pseudo-first-order (Equation (12)) [28], pseudo-second-order (Equation (13)) [29], and Elovich (Equation (14)) [30] kinetic models.

$$\ln(q_e - q_t) = \ln q_e - tK_1 \tag{12}$$

$$\frac{t}{q_t} = \frac{1}{K_2 q_e^2} + \frac{t}{q_e} \tag{13}$$

$$q_t = \frac{1}{\beta} \ln(\alpha \cdot \beta) + \frac{1}{\beta} \ln t \tag{14}$$

where q_t (mg g⁻¹) is the MO amount adsorbed at time t (min), K_1 is the adsorption rate constant of the pseudo-first-order model (min⁻¹), K_2 is the adsorption rate constant of the pseudo-second-order model (g mg⁻¹ min⁻¹), β is the desorption constant (g mg⁻¹), and α is the initial adsorption rate (mg g⁻¹ min⁻¹).

2.8. Thermodynamics

Three common thermodynamic parameters, namely, the standard changes in Gibbs free energy (ΔG°), enthalpy (ΔH°), and entropy (ΔS°) were determined to identify the adsorption type [31]. Therefore, the ΔG° value of MO adsorption by the *Bracteacoccus* sp. at three different temperatures (4, 20, and 36 °C) could be calculated by Equation (15) while keeping the other three factors constant at their optimum values (i.e., $C_o = 10$ mg L⁻¹, adsorbent dose = 0.10 g mL⁻¹, and contact time = 75 min). In addition, the ΔH° and ΔS° values were determined using the Van't Hoff equation (Equation (16)) by plotting $\ln k_d$ vs. $1/T$, and ΔG° could be calculated at a specific temperature using Equation (17) [28].

$$\Delta G^\circ = -RT \ln K_d \tag{15}$$

$$\ln k_d = \Delta S^\circ / R + \frac{\Delta H^\circ}{RT} \tag{16}$$

$$\Delta G^\circ = \Delta H^\circ - T \Delta S^\circ \tag{17}$$

where R is the universal gas constant (8.314 J mol⁻¹ K⁻¹), T is the absolute temperature in kelvin (K), and K_d is the distribution coefficient, which equals the ratio between the amount of MO dye adsorbed and the MO concentration at equilibrium ($K_d = q_e / C_e$).

2.9. Regeneration

The reusability of an adsorbent is a significant factor in reducing the cost of the removal process [32]. Therefore, the *Bracteacoccus* sp. used in the current study was reused up to five times after its separation from an aqueous solution by centrifugation and washing for three times with distilled water.

3. Results

3.1. UV-Vis Analysis

The MO concentration before and after treatment with the *Bracteacoccus* sp. could be easily quantified using UV-vis spectrophotometry. Herein, the mixture containing the MO dye solution and the *Bracteacoccus* sp. was left on the lab bench in the dark for a sufficient contact time of 75 min. Then, the mixture was centrifuged, filtered, and analyzed using a UV spectrophotometer in continuous mode in the range of 200–800 nm at 10 nm wavelength intervals. The analysis results are shown in Figure 1, indicating maximum absorbance of MO at 464 nm and a great reduction in the area under the curve at 464 nm for the MO solution after treatment with the *Bracteacoccus* sp. (i.e., the 464 nm peak vanished). In addition, clear changes were observed for the 230 and 270 nm peaks associated with benzene ring absorption, with the 230 nm peak disappearing, and the 270 nm peak becoming broader. These findings could be due to the destruction of the azo bond in the MO molecules and the formation of intermediate compounds comprising benzene rings [33]. Another crucial observation was that the color of the MO solution that initially was reddish orange gradually changed after the addition of the *Bracteacoccus* sp., and the solution became entirely colorless after 75 min. Therefore, the decolorization of the MO solution by the *Bracteacoccus* sp. could occur as a result of both degradation and sorption processes (binding of the dye molecules by functional groups such as hydroxyl, carboxylate, phosphate, amino, and sulfate groups on the algal surface) [19].

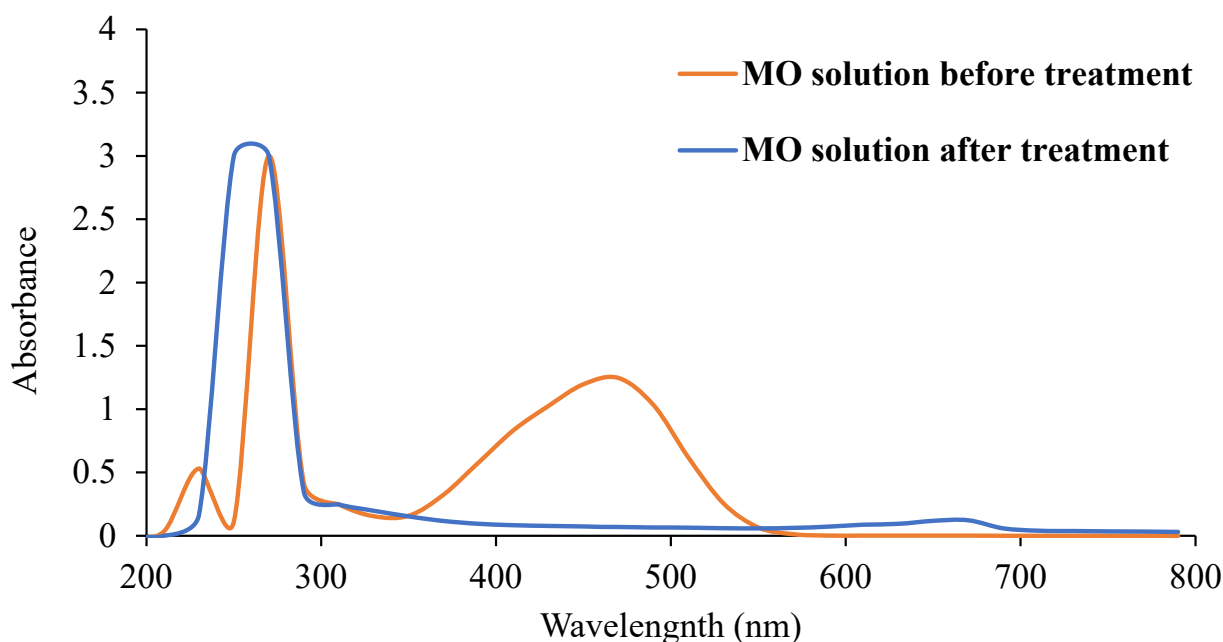


Figure 1. UV-Vis absorption spectra of the MO solution before and after treatment with the *Bracteacoccus* sp. after 75 min of contact time. Inset: a microscope view of the *Bracteacoccus* sp. after absorption of the MO dye. The image was taken at 100× magnification.

In addition, a microscopic view of the *Bracteacoccus* sp. before and after the addition of MO dye is shown in Figure 2. Before MO absorption, the surface morphology of the *Bracteacoccus* sp. was clear and homogeneous, but after MO absorption, the surface morphology became rough and heterogenous.

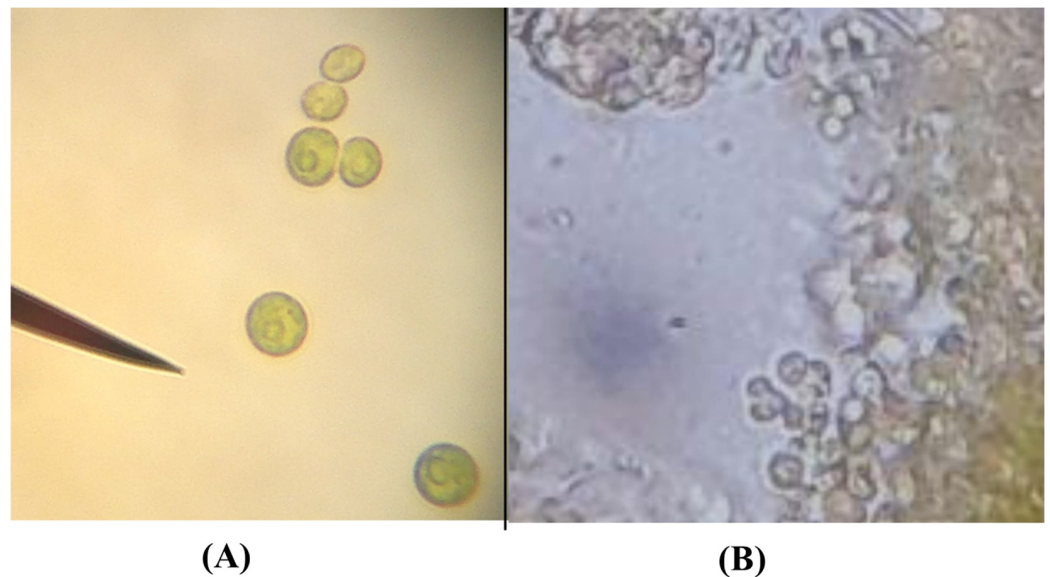


Figure 2. A microscope view of the *Bracteacoccus* sp. before (A) and after (B) the addition of the MO dye. The image was taken at 100× magnification.

3.2. A Comparison between Old, Immobilized Fresh, and Free Fresh *Bracteacoccus* sp.

The *Bracteacoccus* sp. as a biosorbent was used in three statuses, namely, old, immobilized fresh, and free fresh, to investigate its ability to remove the MO dye from aqueous solutions. Based on Figure 3, the free fresh *Bracteacoccus* sp. achieved the highest removal efficiency of MO (97%) from aqueous solutions, followed by the immobilized fresh (85%) and the old (71%) *Bracteacoccus* sp., respectively. This behavior may be due to the high ability of the free fresh *Bracteacoccus* sp. to interact with the MO dye molecules. In contrast, the immobilized fresh *Bracteacoccus* sp. showed a lower removal efficiency because the *Bracteacoccus* sp. molecules were shielded on the beads, which hindered the direct interaction between the MO molecules and the *Bracteacoccus* sp., resulting in a lower efficiency of MO removal. The old *Bracteacoccus* sp. achieved the lowest removal efficiency, as its removal activity was lower, and that adversely reflected on its ability to remove MO from the aqueous solutions.



Figure 3. Old, immobilized fresh, and free fresh *Bracteacoccus* sp. algae for MO dye removal from aqueous solutions. The error bars represent the standard deviation of a triplicate analysis. (C_o of MO = 10 mg L⁻¹, adsorbent dose = 0.10 g mL⁻¹, contact time = 75 min, temperature = 20 °C).

3.3. Optimization of Experimental Factors Using a BBD

The results of the experiments are listed in Table 4. The analysis of the experimental data related to MO dye removal using the free fresh *Bracteacoccus* sp. was achieved using Design Expert version 8, which provided a plot for each factor, displayed in Figure 4. In addition, 3D plots, including illustrations of the interactive effects of the experimental variables, are shown in Figure 5. The effects of these experimental factors can be explained in more detail as follows.

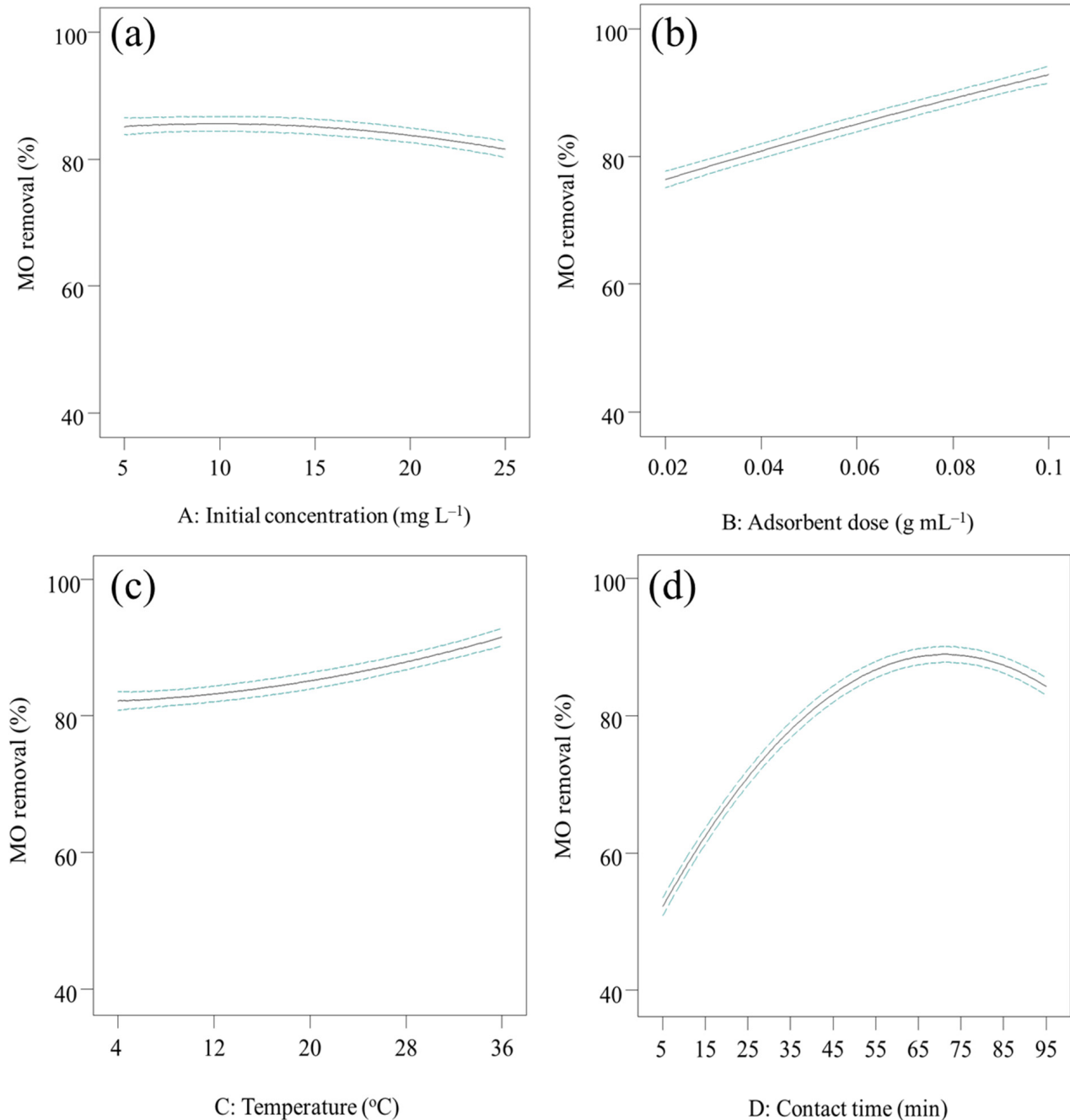


Figure 4. Experimental design to determine the effect of each factor, i.e., initial MO concentration (a), adsorbent dose (b), temperature (c), and contact time (d) on MO removal %.

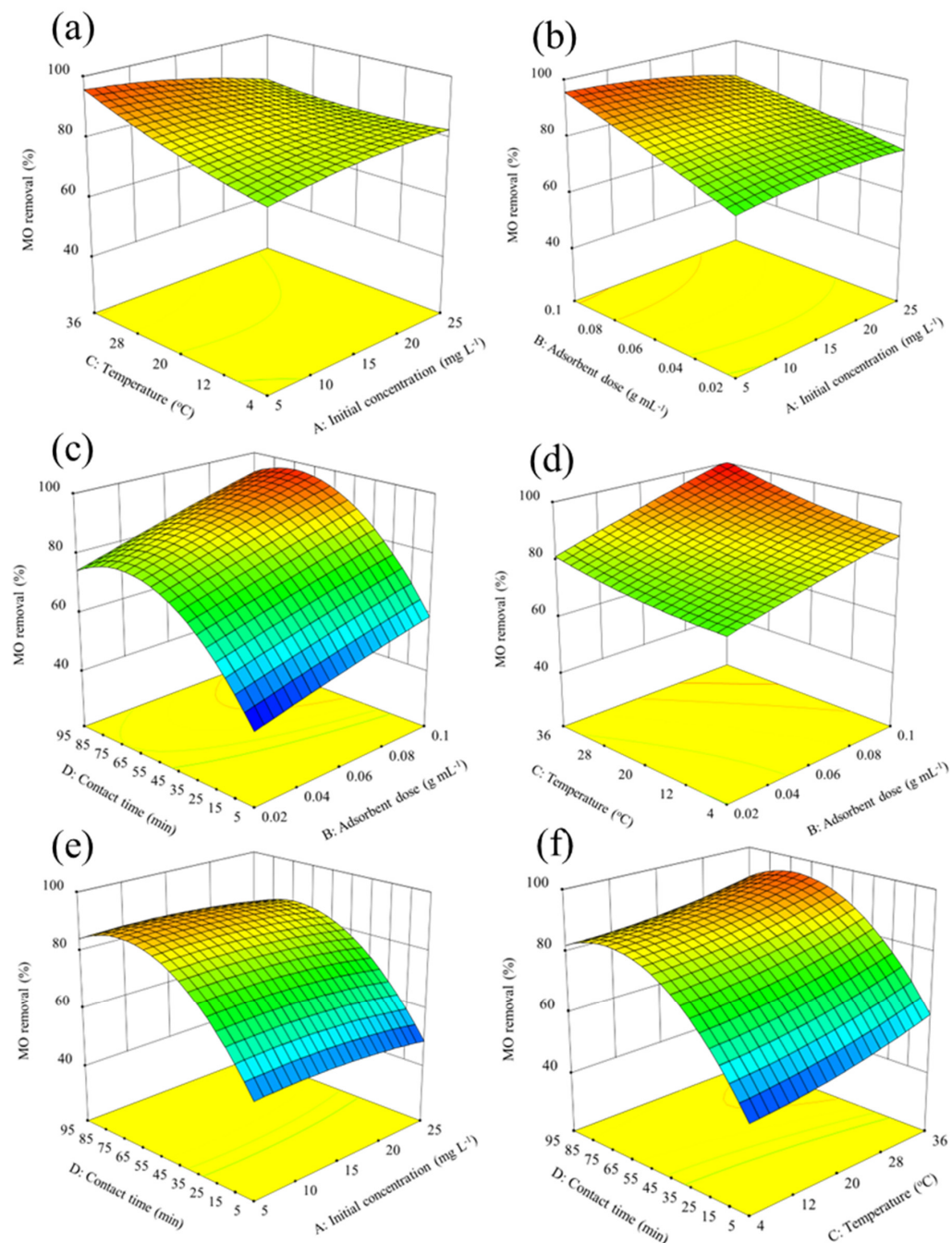


Figure 5. 3D surface plots of MO removal by the *Bracteacoccus* sp. showing the interactive effects of the four factors (initial MO concentration (a,b,e), adsorbent dose (b–d), temperature (a,d,f), and contact time (c,e,f)).

Table 4. Responses are presented as removal % values for the experiments listed in Table 3.

Exp. #	Response (Removal %)	Exp. #	Response (Removal %)
1	76	16	80
2	52	17	76
3	44	18	96
4	83	19	85
5	85	20	86
6	48	21	86
7	94	22	77
8	86	23	60

Table 4. Cont.

Exp. #	Response (Removal %)	Exp. #	Response (Removal %)
9	48	24	99
10	82	25	80
11	75	26	91
12	60	27	89
13	84	28	74
14	84	29	86
15	96		

3.4. Effect of the Initial MO Concentration

Figure 4a shows the effect of the initial MO concentration on the removal percentage of MO dye from aqueous solutions. Clearly, an increase in the initial concentration of MO in the range of 5–15 mg L⁻¹ did not lead to any significant changes in removal %, and the MO removal efficiency (~85%) remained approximately constant. In contrast, a slight decrease in removal % was observed when the MO concentration was in the range of 15–25 mg L⁻¹, which might be due to the saturation of the active sites onto the adsorbent surface by the adsorbate molecules [34]. In addition, the interactive effect between the initial MO concentration and temperature, adsorbent dose, and contact time is shown in Figure 5a,b,e, respectively. The general trend indicated that a decrease in the MO concentration in the presence of a higher adsorbent dose, a higher temperature, and a longer contact time up to 75 min increased the removal of MO dye. Similar trends were described for MO removal in previous studies [35,36].

3.5. Effect of the Adsorbent Dose

The adsorbent dose has a clear effect on both the process cost and the removal % [7]. Therefore, studying the effect of the adsorbent dose to determine the optimal adsorbent dose is an essential step in the optimization process. In Figure 4b, the removal % of MO increases from 77 to 94% with an increasing adsorbent dose from 0.02 to 0.10 g mL⁻¹. This can be attributed to the increase in available sites on the adsorbent, as the adsorbent dose increases [37]. In contrast, the adsorption capacity decreases from 3.45 to 0.9 mg g⁻¹ with an increasing adsorbent dose from 0.02 to 0.10 g. This behavior is due to the fact that the adsorption sites remain unsaturated during adsorption, and there is a less than proportional increase in adsorption due to the lower adsorptive capacity of the adsorbent, though the amount of adsorbent is increased [38]. These results are in agreement with results reported in previous studies [39,40].

3.6. Effect of the Temperature

The temperature affects the chemical composition of a solution, as an increase or a decrease in temperature may increase or decrease the adsorption % [41]. Based on Figure 4c, an increase in temperature from 4 to 36 °C increased the removal % of MO dye from 81 to 90%. This behavior is also shown in Figure 5a,d,f to explain the interactive effect between temperature and the remaining three factors (initial MO concentration, adsorbent dose, and contact time). In general, increasing the temperature up to 36 °C in the presence of a higher adsorbent dose and with sufficient contact time resulted in a high removal of MO from the aqueous solutions. This behavior could be due to several reasons, accompanied by high temperatures, which are (i) the increasing swelling of the dye molecules into the adsorbent structure [42]; (ii) the increasing solubility of the dye; (iii) the increasing collisions between the adsorbent and the adsorbate molecules; (iv) the increasing pore size in the adsorbent [43]. This finding related to the effect of temperature on MO removal is similar in trend to that reported in previous studies for MO removal using Zn-Al layered double hydroxide [42] and *Bacillus stratosphericus* SCA1007 [37].

3.7. Effect of the Contact Time

Figure 4d shows the influence of the contact time on MO removal from aqueous media using the *Bracteacoccus* sp. The removal % was low in the beginning (~40%), then it gradually started to increase, reaching the maximum removal (~90%) after 75 min. Initially, the number of available sites of adsorption was large; therefore, the adsorption rate was large, but with the time passing, these adsorptive sites became saturated, and the adsorption rate decreased; a plateau was observed at equilibrium [44]. In addition, the interactive effect between the contact time, adsorbent dose, initial MO concentration, and temperature is shown in Figure 5c,e,f.

3.8. Analysis of Variance (ANOVA)

In fact, the F-value and *p*-value are crucial to determining the significance of the used model, and a model with a high F-value and a low *p*-value (<0.05) is significant [45]. The results of the ANOVA analysis of the surface quadratic model for MO removal using the *Bracteacoccus* sp. are listed in Table 5, which evidently indicates a high F-value (286.71), a low *p*-value (<0.0001), and a non-significant lack of fit. Adequate precision, which represents the ratio of signal to noise, had a value of 62.028, indicating a desirable ratio (i.e., an adequate signal), being higher than 4 [46]. In addition, the adjusted R² of 0.9930 was in reasonable agreement with the predicted R² of 0.9815, with a difference of less than 0.2. Therefore, the quadratic model used in the current study is valid.

Considering the effects of the different factors, the following equation can be used to determine the predicted value of the removal % of MO given the values of the experimental factors:

$$\begin{aligned}
 \text{MO removal} = & + 17.83024 \\
 & + 1.26629 \times \text{Initial concentration} \\
 & + 272.75347 \times \text{Adsorbent dose} \\
 & + 0.34388 \times \text{Temperature} \\
 & + 1.18298 \times \text{Contact time} \\
 & - 6.81250 \times \text{Initial concentration} \times \text{Adsorbent dose} \\
 & - 0.025781 \times \text{Initial concentration} \times \text{Temperature} \\
 & - 6.77242 \times 10^{-18} \times \text{Initial concentration} \times \text{Contact time} \\
 & + 2.14844 \times \text{Adsorbent dose} \times \text{Temperature} \\
 & + 0.55556 \times \text{Adsorbent dose} \times \text{Contact time} \\
 & - 1.25000 \times 10^{-3} \times \text{Temperature} \times \text{Contact time} \\
 & - 0.017342 \times \text{Initial concentration}^2 \\
 & - 302.60417 \times \text{Adsorbent dose}^2 \\
 & + 6.70247 \times 10^{-3} \times \text{Temperature}^2 \\
 & - 8.35021 \times 10^{-3} \times \text{Contact time}^2
 \end{aligned}$$

Table 5. ANOVA analysis of the surface quadratic model for MO removal using green microalgae.

Source	Sum of Squares	df	Mean Square	F Value	<i>p</i> -Value	Prob > F
Model	6347.89	14	453.42	286.71	<0.0001	significant
A—Initial concentration	38.16	1	38.16	24.13	0.0002	
B—Adsorbent dose	806.88	1	806.88	510.21	<0.0001	
C—Temperature	261.33	1	261.33	165.25	<0.0001	
D—Contact time	3084.81	1	3084.81	1950.62	<0.0001	
AB	29.70	1	29.70	18.78	0.0007	
AC	68.06	1	68.06	43.04	<0.0001	
AD	0.000	1	0.000	0.000	1.0000	
BC	7.56	1	7.56	4.78	0.0462	
BD	4.00	1	4.00	2.53	0.1341	
CD	3.24	1	3.24	2.05	0.1743	

Table 5. Cont.

Source	Sum of Squares	df	Mean Square	F Value	p-Value Prob > F	
A ²	19.51	1	19.51	12.33	0.0035	
B ²	1.52	1	1.52	0.96	0.3435	
C ²	19.10	1	19.10	12.08	0.0037	
D ²	1854.62	1	1854.62	1172.73	<0.0001	
Residual	22.14	14	1.58			
Lack of Fit	19.87	10	1.99	3.50	0.1195	not significant
Pure Error	2.27	4	0.57			
Cor Total	6370.03	28				

3.9. Desirability Function

The desirability function is used as an optimization method; the desirability range is 0–1 (1 is the favored value of the response, while 0 means that the response is far from the accepted one) [47]. Figure 6 shows the optimal predicted values of the experimental variables to obtain the best response (removal %). The results of the desirability function are shown in Figure 6, where the maximum response is displayed with all experimental factors varying in the indicated ranges (i.e., $C_0 = 5\text{--}25\text{ mg L}^{-1}$, temperature = $4\text{--}36\text{ }^\circ\text{C}$, and contact time = $5\text{--}95\text{ min}$). Consequently, the maximum removal of MO (99%) could be achieved at the predicted values of 10 mg L^{-1} as the initial MO concentration, 0.10 g L^{-1} as the adsorbent dose, $20\text{ }^\circ\text{C}$, and 75 min of contact time. These predicted values were experimentally tested in triplicate, and the MO removal was 97%, which indicated that the experimental result was in agreement with the predicted value, with a 2% relative error. Thus, these optimum conditions were used in the subsequent isotherm, kinetic, and thermodynamic experiments.

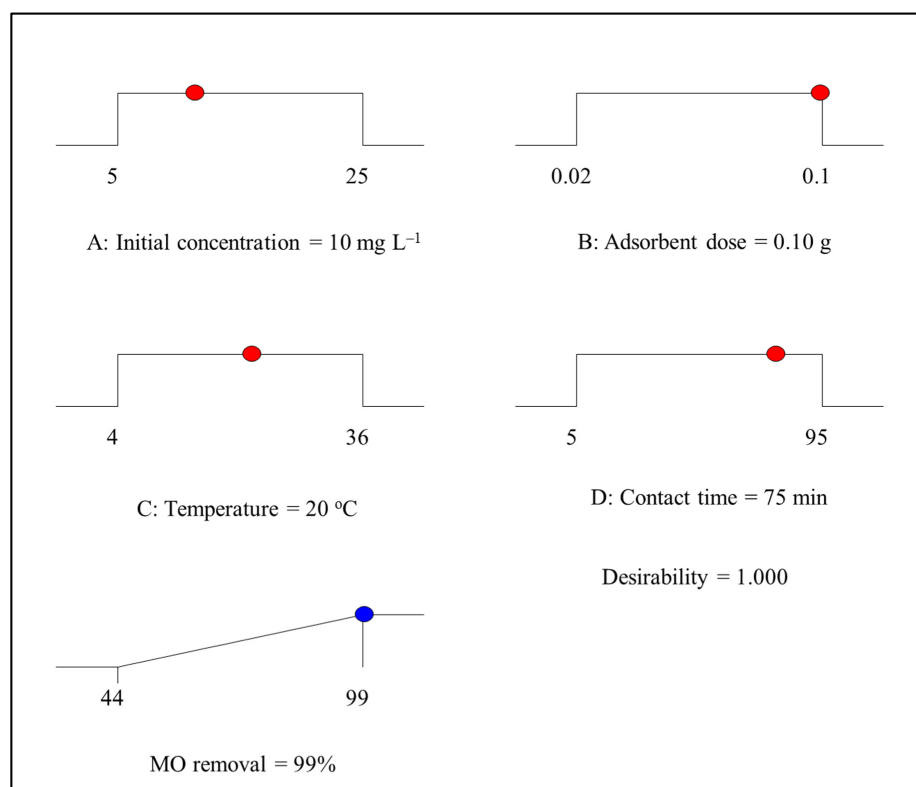


Figure 6. Ramps of desirability for the optimization of the experimental variables (initial MO concentration, adsorbent dose, temperature, and contact time) in MO removal from aqueous solutions by the *Bracteacoccus* sp.

3.10. Isotherm Study

The aim of isotherm models is to understand the mechanisms of interaction between adsorbent and adsorbate molecules at constant temperature [48]. Herein, the results of the isotherm study using the Langmuir, Freundlich, D-R, and Temkin isotherm models are shown in Figure 7. Additionally, the calculated values of the isotherm models' parameters are listed in Table 6, where the experimental data obeying the Langmuir and Temkin isotherm model indicated R^2 of > 0.99 and small RMSE values ($RMSE < 1$). Note that the Langmuir isotherm model indicated that the adsorbate (MO dye) molecules were adsorbed onto the homogeneous surface of the adsorbent (the *Bracteacoccus* sp.), forming a monolayer of adsorbate molecules [22]. The value of q_m was 5.4171 mg g^{-1} , B_T was $1.1639 \text{ J mol}^{-1}$, and b_T was $3225.58 \text{ J mol}^{-1}$. Moreover, MO adsorption onto the *Bracteacoccus* sp. algae was favorable ($R_L = 0.07635$, between 0 and 1). These findings are in agreement with the results described in previous studies [4,29]. Considering the D-R mode results, the value of E was $2.7671 \text{ J mol}^{-1}$, i.e., $< 8 \text{ J mol}^{-1}$; therefore, MO adsorption by the *Bracteacoccus* sp. can be considered physisorption. The n value in the Freundlich isotherm model was 2.8514 ($n > 1$), which confirmed that the sorption of MO by the *Bracteacoccus* sp. was adequate.

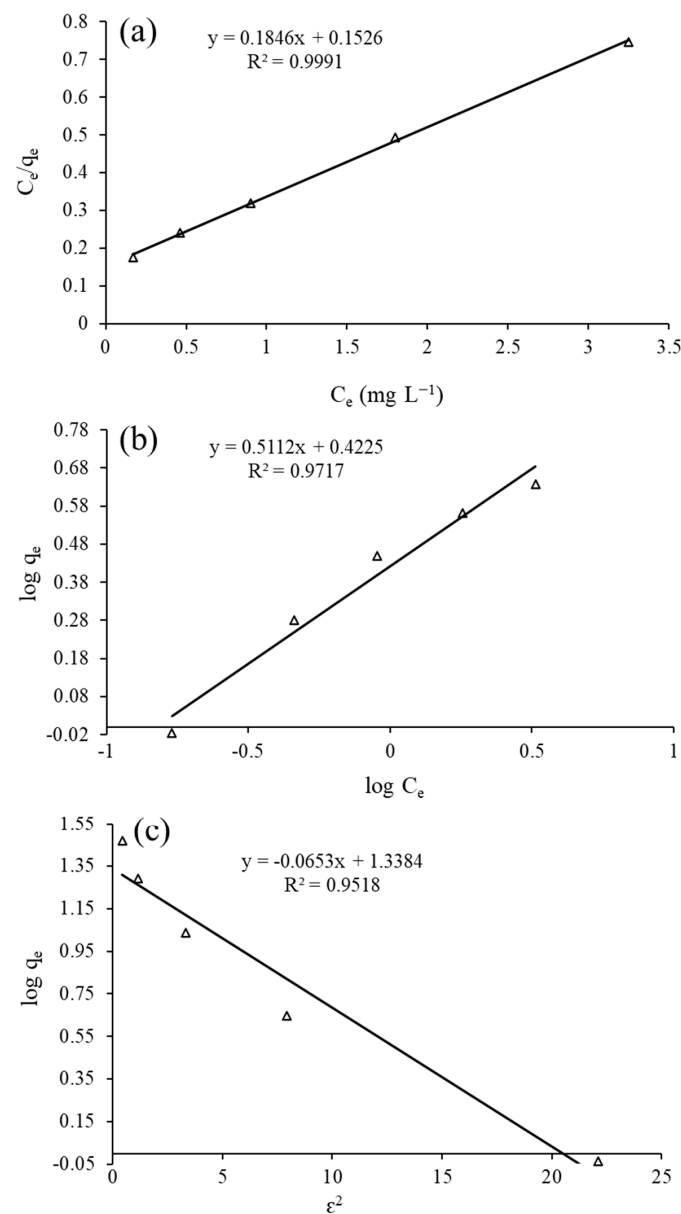


Figure 7. Cont.

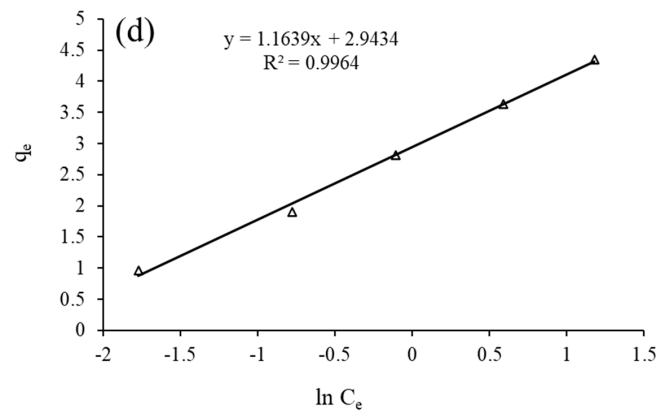


Figure 7. Linear plots of the isotherm models, including (a) Langmuir, (b) Freundlich, (c) D–R, and (d) Temkin isotherm models for MO adsorption using the *Bracteacoccus* sp.

Table 6. The values of the isotherm terms of the Langmuir, Freundlich, D–R, and Temkin isotherm models for MO dye adsorption using the *Bracteacoccus* sp.

Isotherm Model	Parameters	Values
Langmuir	q_e^{max} (mg g ⁻¹)	5.4171
	K_L (L mg ⁻¹)	1.2067
	R_L	0.07635
	R^2	0.9991
	RMSE	0.04197
Freundlich	K_f ((mg g ⁻¹)(L mg ⁻¹) ^{1/n})	2.3977
	n	2.8514
	R^2	0.9717
D-R	RMSE	61.0529
	Q_m (mg g ⁻¹)	3.8129
	K_D (mol ² /kJ ²)	0.0653
	E (J mol ⁻¹)	2.7671
	R^2	0.9518
Temkin	RMSE	14.4135
	A_T (L g ⁻¹)	33.869
	B_T (J mol ⁻¹)	1.1639
	b_T (J mol ⁻¹)	3225.58
	R^2	0.9946
	RMSE	0.07198

3.11. Kinetic Study

The kinetic study helped to understand the adsorption mechanism, calculate the adsorption rate constant, and evaluate the adsorption capacity. The results obtained after applying the pseudo–first–order, pseudo–second–order, and Elovich kinetic are depicted in Figure 8, and the calculated values of the corresponding kinetic parameters are summarized in Table 7. Obviously, the experimental data were best fitted by the pseudo-second-order model ($R^2 = 0.9999$ and $RMSE = 0.0457$). This finding is in agreement with previous studies of MO removal using *Oedogonium subplagiostomum* AP1 [12] and *Chlorella* species [13]. The adsorption capacity was 2.0588 mg g⁻¹, and the rate constant K_2 was 0.0766 g mg⁻¹ min⁻¹.

Compared to the pseudo-second-order kinetic model, the Elovich kinetic model achieved a lower fit ($R^2 = 0.9363$) for MO adsorption onto the *Bracteacoccus* sp., indicating that the MO adsorption mechanism diverged from chemisorption [49]. Among these kinetic models, the pseudo-first-order kinetic model provided the lowest value.

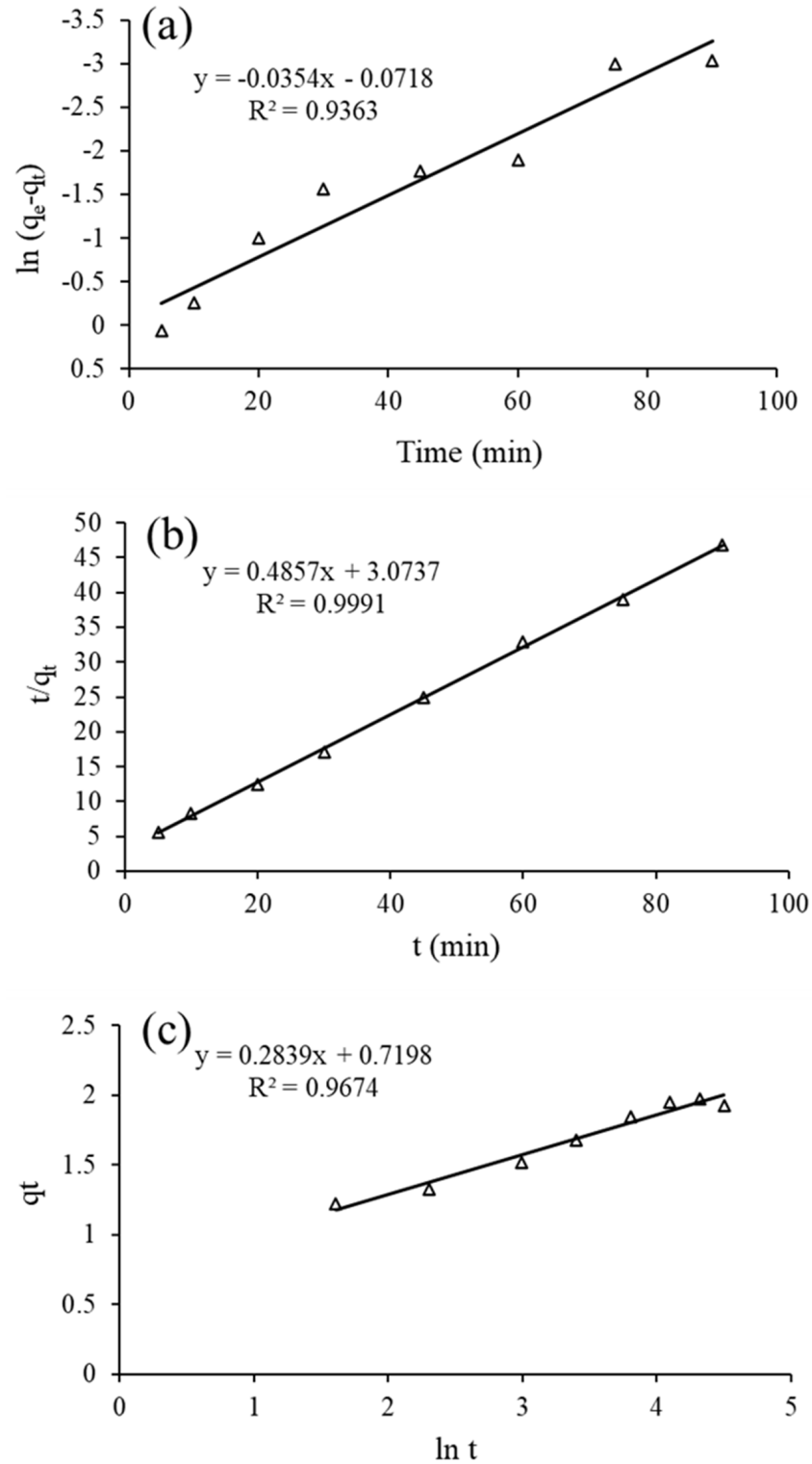


Figure 8. Plots of pseudo-first-order (a), pseudo-second-order (b), and Elovich (c) kinetic models for MO adsorption onto the *Bracteacoccus* sp. ($C_0 = 10 \text{ mg L}^{-1}$, adsorbent dose = 0.1 g, and temperature = 20 °C).

Table 7. The calculated values of parameters in pseudo-first-order, pseudo-second-order, and Elovich kinetic models. ($C_0 = 10 \text{ mg L}^{-1}$, adsorbent dose = 0.1 g, and temperature = 20 °C).

Kinetic Model	Parameters	Values
Pseudo-first-order	$q_e \text{ (mg g}^{-1}\text{)}$	0.9307
	$K_1 \text{ (min}^{-1}\text{)}$	0.0354
	R^2	0.9363
	RMSE	2.0556
Pseudo-second-order	$q_e \text{ (mg g}^{-1}\text{)}$	2.0588
	$K_2 \text{ (g mg}^{-1} \text{ min}^{-1}\text{)}$	0.0766
	R^2	0.9991
	RMSE	0.04569
Elovich	$\beta \text{ (g mg}^{-1}\text{)}$	66.6667
	$\alpha \text{ (mg g}^{-1} \text{ min}^{-1}\text{)}$	5.1476×10^{11}
	R^2	0.9674
	RMSE	1.0074

Algae mainly consist of polysaccharides, including three groups, namely, polycolloids, alginates, and carrageenans, which have a key role in binding pollutants to the algal surface [50]. For example, the *Bracteacoccus* sp., a green alga, consists of protein and cellulose groups bonded to polysaccharides in the wall of cells [51]. Therefore, the adsorptive removal of a pollutant (e.g., MO) from aqueous solutions using a biosorbent (e.g., the *Bracteacoccus* sp.) can occur through two approaches as follows: (i) surface sorption, in which the adsorbate molecules migrate from the bulk aqueous solution toward a surrounding layer on the adsorbent surface, then establishing a direct interaction with the functional groups on the adsorbate surface; (ii) interstitial sorption, where the adsorbate molecules enter the pores in the adsorbent [52]. Consequently, the proposed mechanism for dye adsorption onto green microalgae (e.g., the *Bracteacoccus* sp.) includes the interaction between the functional groups (e.g., amine, hydroxyl, carbonyl, carboxyl, phosphate, and sulfate) of the green microalgae and the dye molecules [53]. Thus, the biosorption of MO may occur via H-bonding, electrostatic, ion exchange, and π - π interactions [54].

3.12. Thermodynamic Study

The thermodynamic study of the current work was carried out at three different temperatures: 4 °C (277 K), 20 °C (293 K), and 36 °C (309 K). The thermodynamic results are depicted in Figure 9, and the values of the thermodynamic parameters are listed in Table 8. The positive ΔH° and the negative ΔG° values indicated that MO adsorption by the *Bracteacoccus* sp. was endothermic and spontaneous, respectively. The absolute value of ΔG° increased with increasing temperature, and the maximum value of ΔG° was $-13.909 \text{ KJ mol}^{-1}$, in the range from 0 to -20 KJ mol^{-1} ; therefore, MO adsorption by the *Bracteacoccus* sp. is physisorption [55]. In addition, the positive value of ΔS° indicated an increase in entropy (randomness) at the solid–solution interface during MO adsorption [56]. Similar trends were reported in previous studies of MO adsorption using activated carbon [57] and magnetic resin in chitosan microspheres [55].

Table 8. The calculated values of thermodynamic parameters for MO removal using the *Bracteacoccus* sp. ($C_0 = 10 \text{ mg L}^{-1}$, adsorbent dose = 0.1 g, and contact time = 75 min).

$\Delta H^\circ \text{ (KJ/mol)}$	$\Delta S^\circ \text{ (KJ/mol)}$	$\Delta G^\circ \text{ (KJ/mol)}$		
		277 k	293 k	309 k
+49.469	+0.205	-7.345	-10.627	-13.909

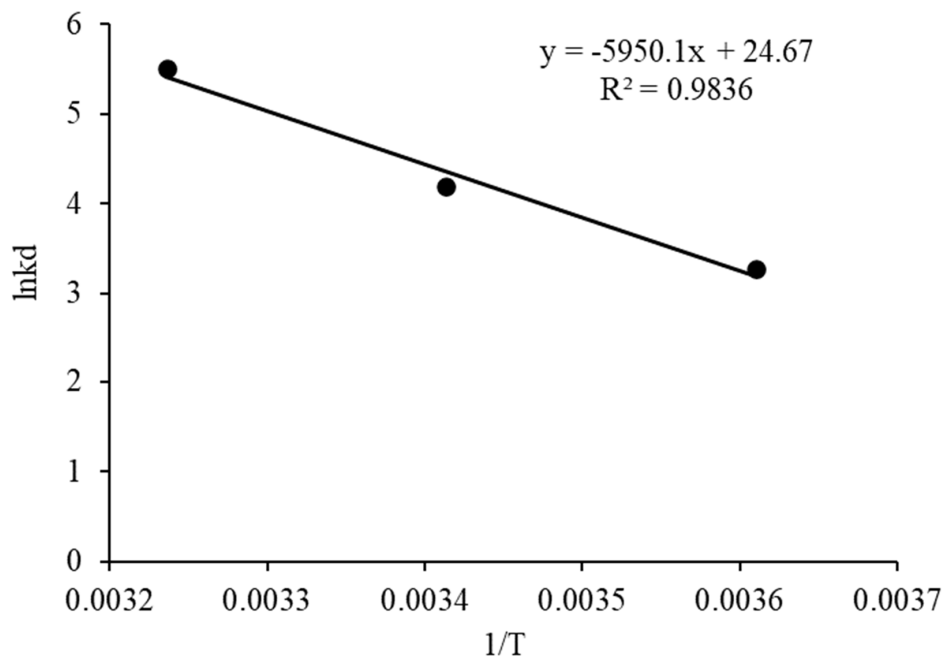


Figure 9. The plot of $\ln K_d$ versus $1/T$ for MO adsorption by the *Bracteaococcus* sp. ($C_0 = 10 \text{ mg L}^{-1}$, adsorbent dose = 0.1 g, and contact time = 75 min).

3.13. Regeneration

The reusability of the *Bracteaococcus* sp. is an important property that should be investigated to estimate the cost effectiveness of MO removal from aqueous solutions, especially if the current procedure is applied on a large scale. Therefore, five regeneration and reusability cycles of the immobilized and free fresh *Bracteaococcus* sp. were performed to remove MO from aqueous solutions. The results are shown in Figure 10 and indicate that the *Bracteaococcus* sp. can be reused up to five times without any significant deficiency in the removal efficiency of MO from aqueous solutions, considering that the free fresh *Bracteaococcus* sp. removed approximately 96% of MO from the aqueous solutions, while the removal efficiency of the immobilized alga was lower (~83%).

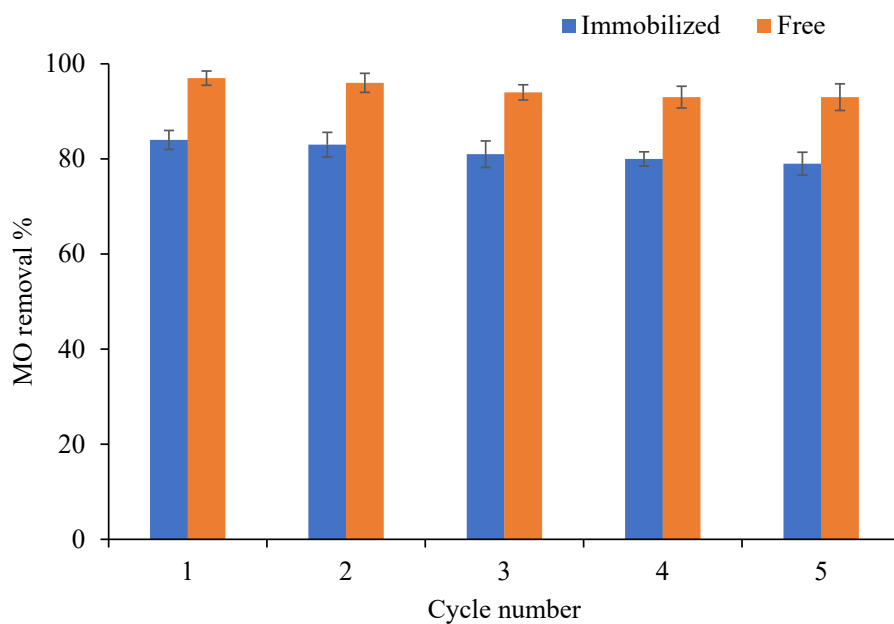


Figure 10. Number of regeneration cycles of the *Bracteaococcus* sp. for MO removal from aqueous solutions.

3.14. Comparison with Other Adsorbents

Based on previous studies, some biosorbents such as algae (e.g., *Fucus vesiculosus* [11], *Chlorella* species [13], and *Oedogonium subplagiostomum* AP1 [12]) and microbial cultures (e.g., of *M. yunnaenensis* [58] and *Bacillus stratosphericus* SCA1007 [37] and anaerobic–aerobic microbial culture/coconut fiber systems [59]) are effective in removing/degrading MO dye (Table 9). Algae (e.g., *Fucus vesiculosus*) have a reasonable efficiency (50%) of MO removal in 60 min. In addition, the highest MO removal (>95%) was observed with *Oedogonium subplagiostomum* AP1, *M. yunnaenensis*, and *Bacillus stratosphericus* SCA1007, but the required contact time was relatively high and varied based on the adsorbent used, in the following order: *Oedogonium subplagiostomum* AP1 (5.5 days) > *M. yunnaenensis* (5.0 days) > *Bacillus stratosphericus* SCA1007 (1/2 days).

Table 9. Some biosorbents used for MO removal from aqueous solutions.

Biosorbent	Experimental Conditions	q_m (mg g ⁻¹)	R%	Ref.
Alga (<i>Fucus vesiculosus</i>)	10 mL of a 60 mg L ⁻¹ MO solution, pH = 7.0, 3 g L ⁻¹ of adsorbent dose, and 60 min of contact time	0.10	50%	[11]
<i>Chlorella</i> species	1.0–2.2 mg L ⁻¹ initial MO concentration and 0.7 g of adsorbent in 50 mL of aqueous solution	0.74–0.27	-	[13]
Alga (<i>Oedogonium subplagiostomum</i> AP1)	500 mg L ⁻¹ initial MO concentration, pH = 6.5, 400 mg L ⁻¹ algal dose, and 5.5 days of contact time	1213	97%	[12]
Microbial culture (bacterial strain, <i>M. yunnaenensis</i>)	100 mL of a 100 mg L ⁻¹ MO solution, pH 7.0, 3 mL (culture), and 5.0 days of contact time	-	98%	[58]
Microbial culture (<i>Bacillus stratosphericus</i> SCA1007)	100 mL of a 150 mg L ⁻¹ MO solution, optical density 1.0 (λ_{max} = 600 nm, 1.50×10^6 cells mL ⁻¹), pH 7.0, T = 35 °C, 3 mL (culture), and 12 h of contact time	-	100%	[37]
Biofilm reactor containing anaerobic–aerobic microbial culture/coconut fiber	3 L reactor with anaerobic–aerobic biofilm (7.2 cm diameter × 75 cm height) filled with 1 L of coconut fiber, 200 mg L ⁻¹ initial MO concentration, contact time of 36 days with aeration for 24 h	1.20	81%	[59]
Green microalga (<i>Bracteacoccus</i> sp.)	20 mL of MO solution (10 mg L ⁻¹), 0.10 g L ⁻¹ adsorbent dose, 20 °C temperature, and 75 min of contact time	5.42	97%	The current study

In contrast, the *Bracteacoccus* sp. used in the current study needed a shorter contact time (~75 min) to remove 97% of MO dye from an aqueous solution. Therefore, the *Bracteacoccus* sp. is an effective biosorbent, able to extensively remove MO dye from an aqueous medium within a relatively short time.

4. Conclusions

The *Bracteacoccus* sp. (green microalga) showed a high efficiency (97%) of MO dye removal from aqueous solutions in a relatively short time (75 min). The Box–Behnken design (BBD)-based response surface methodology (RSM) is a useful mathematical tool that can be successfully used to optimize MO removal from aqueous solutions and reduce the operation cost. Experimental factors such as initial MO concentration, adsorbent dose, temperature, and contact time have clear effects on MO removal using the *Bracteacoccus* sp. MO is adsorbed and forms a monolayer onto the *Bracteacoccus* sp. surface in an endothermic and spontaneous process. Compared to old and immobilized fresh *Bracteacoccus* sp. algae, free fresh *Bracteacoccus* sp. algae showed a higher efficiency of MO removal from aqueous solutions. The mechanism of MO removal using the *Bracteacoccus* sp. was found to include both sorption and degradation processes, where MO is converted to smaller compounds. The *Bracteacoccus* sp. can be regenerated and reused up to five times to remove MO from aqueous solutions with a high removal efficiency. Moreover, the removal process of MO from an aqueous solution using the *Bracteacoccus* sp. has several advantages, such as simplicity, low cost, ease of use, and use of an environmentally friendly adsorbent. Thus, the current procedure is a promising method in environmental remediation for protecting

water sources from pollution by synthetic dyes, using an abundant natural biosorbent (e.g., the *Bracteacoccus* sp.).

Supplementary Materials: The following supporting information can be downloaded at: <https://www.mdpi.com/article/10.3390/separations11060170/s1>, Figure S1: ESI/MS spectra of MO solutions before and after treatment by the green microalgae (*Bracteacoccus* sp.); Table S1: Proposed chemical structures based on the ESI/MS spectra of the MO solutions shown in Figure S1 (notice the proposed chemical structures of intermediates derived from MO degradation reported in a previous study [60]).

Author Contributions: Conceptualization, A.A.S. and A.T.A.-F.; methodology, A.A.S., A.T.A.-F. and M.M.I.; software, A.A.S.; validation, A.A.S. and E.A.; formal analysis, A.A.S. and A.T.A.-F.; investigation, A.A.S. and A.T.A.-F.; resources, A.A.S., A.T.A.-F., M.M.I. and E.A.; data curation, A.A.S. and A.T.A.-F.; writing—original draft preparation, A.A.S.; writing—review and editing, A.A.S., A.T.A.-F., M.M.I. and E.A.; visualization, A.A.S. and A.T.A.-F. All authors have read and agreed to the published version of the manuscript.

Funding: This research received no external funding.

Data Availability Statement: The data that support the findings of this study are available from the corresponding author upon reasonable request.

Acknowledgments: The authors thank Al al-Bayt University (Mafraq, Jordan) for providing financial support and laboratory facilities to perform this work.

Conflicts of Interest: The authors declare no conflicts of interest.

References

1. Ahmed, M.A.; Ahmed, M.A.; Mohamed, A.A. Synthesis, Characterization and Application of Chitosan/Graphene Oxide/Copper Ferrite Nanocomposite for the Adsorptive Removal of Anionic and Cationic Dyes from Wastewater. *RSC Adv.* **2023**, *13*, 5337–5352. [[CrossRef](#)] [[PubMed](#)]
2. Aljuaid, A.; Almeahmadi, M.; Alsaiani, A.A.; Allahyani, M.; Abdulaziz, O.; Alsharif, A.; Alsaiani, J.A.; Saih, M.; Alotaibi, R.T.; Khan, I. G-C₃N₄ Based Photocatalyst for the Efficient Photodegradation of Toxic Methyl Orange Dye: Recent Modifications and Future Perspectives. *Molecules* **2023**, *28*, 3199. [[CrossRef](#)] [[PubMed](#)]
3. Hosny, N.M.; Gomaa, I.; Elmahgary, M.G. Adsorption of Polluted Dyes from Water by Transition Metal Oxides: A Review. *Appl. Surf. Sci. Adv.* **2023**, *15*, 100395. [[CrossRef](#)]
4. Wang, K.; Kou, Y.; Wang, K.; Liang, S.; Guo, C.; Wang, W.; Lu, Y.; Wang, J. Comparing the Adsorption of Methyl Orange and Malachite Green on Similar yet Distinct Polyamide Microplastics: Uncovering Hydrogen Bond Interactions. *Chemosphere* **2023**, *340*, 139806. [[CrossRef](#)] [[PubMed](#)]
5. Hasan, I.; Albaeejan, M.A.; Alshayiqi, A.A.; Al-Nafaei, W.S.; Alharthi, F.A. In Situ Hydrothermal Synthesis of Ni_{1-x}MnxWO₄ Nanoheterostructure for Enhanced Photodegradation of Methyl Orange. *Molecules* **2023**, *28*, 1140. [[CrossRef](#)] [[PubMed](#)]
6. Ali, F.; Mehmood, S.; Ashraf, A.; Saleem, A.; Younas, U.; Ahmad, A.; Bhatti, M.P.; Eldesoky, G.E.; Aljuwayid, A.M.; Habila, M.A.; et al. Ag-Cu Embedded SDS Nanoparticles for Efficient Removal of Toxic Organic Dyes from Water Medium. *Ind. Eng. Chem. Res.* **2023**, *62*, 4765–4777. [[CrossRef](#)]
7. Alardhi, S.M.; Fiyadh, S.S.; Salman, A.D.; Adelikhah, M. Prediction of Methyl Orange Dye (MO) Adsorption Using Activated Carbon with an Artificial Neural Network Optimization Modeling. *Heliyon* **2023**, *9*, e12888. [[CrossRef](#)]
8. Iwuozor, K.O.; Ighalo, J.O.; Emenike, E.C.; Ogunfowora, L.A.; Igwegbe, C.A. Adsorption of Methyl Orange: A Review on Adsorbent Performance. *Curr. Res. Green Sustain. Chem.* **2021**, *4*, 100179. [[CrossRef](#)]
9. Yaashikaa, P.R.; Kumar, P.S.; Saravanan, A.; Vo, D.V.N. Advances in Biosorbents for Removal of Environmental Pollutants: A Review on Pretreatment, Removal Mechanism and Future Outlook. *J. Hazard. Mater.* **2021**, *420*, 126596. [[CrossRef](#)]
10. Lin, Z.; Li, J.; Luan, Y.; Dai, W. Application of Algae for Heavy Metal Adsorption: A 20-Year Meta-Analysis. *Ecotoxicol. Environ. Saf.* **2020**, *190*, 110089. [[CrossRef](#)]
11. El-Naggar, N.E.A.; Hamouda, R.A.; Saddiq, A.A.; Alkinani, M.H. Simultaneous Bioremediation of Cationic Copper Ions and Anionic Methyl Orange Azo Dye by Brown Marine Alga *Fucus Vesiculosus*. *Sci. Rep.* **2021**, *11*, 3555. [[CrossRef](#)] [[PubMed](#)]
12. Maruthanayagam, A.; Mani, P.; Kaliappan, K.; Chinnappan, S. In Vitro and In Silico Studies on the Removal of Methyl Orange from Aqueous Solution Using *Oedogonium Subplagiostomum* AP1. *Water Air Soil Pollut.* **2020**, *231*, 232. [[CrossRef](#)]
13. Doshi, H.; Ray, A.; Kothari, I.L.; Gami, B. Spectroscopic and Scanning Electron Microscopy Studies of Bioaccumulation of Pollutants by Algae. *Curr. Microbiol.* **2006**, *53*, 148–157. [[CrossRef](#)] [[PubMed](#)]
14. Rápó, E.; Tonk, S. Factors Affecting Synthetic Dye Adsorption; Desorption Studies: A Review of Results from the Last Five Years (2017–2021). *Molecules* **2021**, *26*, 5419. [[CrossRef](#)] [[PubMed](#)]

15. Saleh, B.; Fathi, R.; Abdalla, M.A.A.; Radhika, N.; Ma, A.; Jiang, J. Optimization and Characterization of Centrifugal-Cast Functionally Graded Al-SiC Composite Using Response Surface Methodology and Grey Relational Analysis. *Coatings* **2023**, *13*, 813. [[CrossRef](#)]
16. Williamson, E.M.; Sun, Z.; Mora-Tamez, L.; Brutchey, R.L. Design of Experiments for Nanocrystal Syntheses: A How-To Guide for Proper Implementation. *Chem. Mater.* **2022**, *34*, 9823–9835. [[CrossRef](#)]
17. Osuchukwu, O.A.; Salihi, A.; Abdullahi, I.; Abdulkareem, B.; Salami, K.A.; Osayamen Etinosa, P.; Nwigbo, S.C.; Mohammed, S.A.; Obada, D.O. A Pedagogical Approach for the Development and Optimization of a Novel Mix of Biowastes-Derived Hydroxyapatite Using the Box-Behnken Experimental Design. *Heliyon* **2024**, *10*, e23092. [[CrossRef](#)] [[PubMed](#)]
18. Song, S.; Hao, C.; Zhang, X.; Zhang, Q.; Sun, R. Sonocatalytic Degradation of Methyl Orange in Aqueous Solution Using Fe-Doped TiO₂ Nanoparticles under Mechanical Agitation. *Open Chem.* **2018**, *16*, 1283–1296. [[CrossRef](#)]
19. Al-Fawwaz, A.T.; Al Shra'ah, A.; Elhaddad, E. Bioremoval of Methylene Blue from Aqueous Solutions by Green Algae (*Bracteacoccus* sp.) Isolated from North Jordan: Optimization, Kinetic, and Isotherm Studies. *Sustainability* **2023**, *15*, 842. [[CrossRef](#)]
20. Hambisa, A.A.; Regasa, M.B.; Ejigu, H.G.; Senbeto, C.B. Adsorption Studies of Methyl Orange Dye Removal from Aqueous Solution Using Anchote Peel-Based Agricultural Waste Adsorbent. *Appl. Water Sci.* **2023**, *13*, 24. [[CrossRef](#)]
21. Asanjarani, N.; Bagtash, M.; Zolgharnein, J. A Comparison between Box–Behnken Design and Artificial Neural Network: Modeling of Removal of Phenol Red from Water Solutions by Nanocobalt Hydroxide. *J. Chemom.* **2020**, *34*, 9. [[CrossRef](#)]
22. Mahdi, A.E.; Ali, N.S.; Kalash, K.R.; Salih, I.K.; Abdulrahman, M.A.; Albayati, T.M. Investigation of Equilibrium, Isotherm, and Mechanism for the Efficient Removal of 3-Nitroaniline Dye from Wastewater Using Mesoporous Material MCM-48. *Prog. Color. Coat.* **2023**, *16*, 387–398. [[CrossRef](#)]
23. Hassaan, M.A.; Yilmaz, M.; Helal, M.; El-Nemr, M.A.; Ragab, S.; El Nemr, A. Isotherm and Kinetic Investigations of Sawdust-Based Biochar Modified by Ammonia to Remove Methylene Blue from Water. *Sci. Rep.* **2023**, *13*, 12724. [[CrossRef](#)] [[PubMed](#)]
24. Shoaib, A.G.M.; Ragab, S.; El Sikaily, A.; Yilmaz, M.; El Nemr, A. Thermodynamic, Kinetic, and Isotherm Studies of Direct Blue 86 Dye Adsorption by Cellulose Hydrogel. *Sci. Rep.* **2023**, *13*, 5910. [[CrossRef](#)] [[PubMed](#)]
25. Deka, J.; Das, H.; Singh, A.; Barman, P.; Devi, A.; Bhattacharyya, K.G. Methylene Blue Removal Using Raw and Modified Biomass *Plumeria Alba* (White Frangipani) in Batch Mode: Isotherm, Kinetics, and Thermodynamic Studies. *Environ. Monit. Assess.* **2023**, *195*, 26. [[CrossRef](#)]
26. Wekoye, J.N.; Wanyonyi, W.C.; Wangila, P.T.; Tonui, M.K. Kinetic and Equilibrium Studies of Congo Red Dye Adsorption on Cabbage Waste Powder. *Environ. Chem. Ecotoxicol.* **2020**, *2*, 24–31. [[CrossRef](#)]
27. Kavcı, E. Adsorption of Direct Red 243 Dye onto Clay: Kinetic Study and Isotherm Analysis. *Desalination Water Treat.* **2021**, *212*, 452–461. [[CrossRef](#)]
28. Zghal, S.; Jedidi, I.; Cretin, M.; Cerneaux, S.; Abdelmouleh, M. Adsorptive Removal of Rhodamine B Dye Using Carbon Graphite/CNT Composites as Adsorbents: Kinetics, Isotherms and Thermodynamic Study. *Materials* **2023**, *16*, 1015. [[CrossRef](#)] [[PubMed](#)]
29. Ahmed, A.S.A.; Sanad, M.M.S.; Kotb, A.; Negm, A.N.R.M.; Abdallah, M.H. Removal of Methyl Red from Wastewater Using a NiO@Hyphaene Thebaica Seed-Derived Porous Carbon Adsorbent: Kinetics and Isotherm Studies. *Mater. Adv.* **2023**, *4*, 2981–2990. [[CrossRef](#)]
30. Thamer, B.M.; Al-aizari, F.A.; Abdo, H.S. Enhanced Adsorption of Textile Dyes by a Novel Sulfonated Activated Carbon Derived from Pomegranate Peel Waste: Isotherm, Kinetic and Thermodynamic Study. *Molecules* **2023**, *28*, 7712. [[CrossRef](#)]
31. Dutta, S.K.; Amin, M.K.; Ahmed, J.; Elias, M.; Mahiuddin, M. Removal of Toxic Methyl Orange by a Cost-Free and Eco-Friendly Adsorbent: Mechanism, Phytotoxicity, Thermodynamics, and Kinetics. *S. Afr. J. Chem. Eng.* **2022**, *40*, 195–208. [[CrossRef](#)]
32. Cheng, Z.; Feng, K.; Su, Y.; Ye, J.; Chen, D.; Zhang, S.; Zhang, X.; Dionysiou, D.D. Novel Biosorbents Synthesized from Fungal and Bacterial Biomass and Their Applications in the Adsorption of Volatile Organic Compounds. *Bioresour. Technol.* **2020**, *300*, 122705. [[CrossRef](#)] [[PubMed](#)]
33. Shen, T.; Jiang, C.; Wang, C.; Sun, J.; Wang, X.; Li, X. A TiO₂ Modified Abiotic–Biotic Process for the Degradation of the Azo Dye Methyl Orange. *RSC Adv.* **2015**, *5*, 58704–58712. [[CrossRef](#)]
34. Hii, H.T. Adsorption Isotherm and Kinetic Models for Removal of Methyl Orange and Remazol Brilliant Blue R by Coconut Shell Activated Carbon. *Trop. Aquat. Soil. Pollut.* **2021**, *1*, 1–10. [[CrossRef](#)]
35. Akansha, K.; Chakraborty, D.; Sachan, S.G. Decolorization and Degradation of Methyl Orange by *Bacillus Stratosphericus* SCA1007. *Biocatal. Agric. Biotechnol.* **2019**, *18*, 101044. [[CrossRef](#)]
36. Shi, X.; Zhang, X.; Ma, L.; Xiang, C.; Li, L. TiO₂-Doped Chitosan Microspheres Supported on Cellulose Acetate Fibers for Adsorption and Photocatalytic Degradation of Methyl Orange. *Polymers* **2019**, *11*, 1293. [[CrossRef](#)] [[PubMed](#)]
37. Nouaa, S.; Aziam, R.; Benhiti, R.; Carja, G.; Iaich, S.; Zerbet, M.; Chiban, M. Synthesis of LDH/Alginate Composite Beads as a Potential Adsorbent for Phosphate Removal: Kinetic and Equilibrium Studies. *Chem. Pap.* **2023**, *77*, 6689–6705. [[CrossRef](#)]
38. Chiban, M.; Carja, G.; Lehtu, G.; Sinan, F. Equilibrium and Thermodynamic Studies for the Removal of As(V) Ions from Aqueous Solution Using Dried Plants as Adsorbents. *Arab. J. Chem.* **2016**, *9*, S988–S999. [[CrossRef](#)]
39. Ramutshatsha-Makhwedzha, D.; Mavhungu, A.; Moropeng, M.L.; Mbaya, R. Activated Carbon Derived from Waste Orange and Lemon Peels for the Adsorption of Methyl Orange and Methylene Blue Dyes from Wastewater. *Heliyon* **2022**, *8*, e09930. [[CrossRef](#)]
40. Djezar, H.; Rida, K.; Salhi, M. Efficient Adsorbent for the Removal of Methyl Orange and Congo Red by Calcined Zn-Al Layered Double Hydroxide. *Inorg. Nano-Met. Chem.* **2022**, *52*, 161–172. [[CrossRef](#)]

41. Khalil, M.; Hanif, M.A.; Rashid, U.; Ahmad, J.; Alsalmeh, A.; Tsubota, T. Low-Cost Novel Nano-Constructed Granite Composites for Removal of Hazardous Terasil Dye from Wastewater. *Environ. Sci. Pollut. Res.* **2023**, *30*, 81333–81351. [[CrossRef](#)] [[PubMed](#)]
42. Sarfraz, S.; Ameer, S.; Javed, M.; Iqbal, S.; Aljazzar, S.O.; Zahra, M.; Amin, S.; Shah, K.H.; Abourehab, M.A.S.; Elkaeed, E.B.; et al. Removal of Hexavalent Chromium Ions Using Micellar Modified Adsorbent: Isothermal and Kinetic Investigations. *RSC Adv.* **2022**, *12*, 23898–23911. [[CrossRef](#)] [[PubMed](#)]
43. Etemadinia, T.; Allahrasani, A.; Barikbin, B. ZnFe₂O₄@SiO₂@Tragacanth Gum Nanocomposite: Synthesis and Its Application for the Removal of Methylene Blue Dye from Aqueous Solution. *Polym. Bull.* **2019**, *76*, 6089–6109. [[CrossRef](#)]
44. Imessaoudene, A.; Cheikh, S.; Hadadi, A.; Hamri, N.; Bollinger, J.C.; Amrane, A.; Tahraoui, H.; Manseri, A.; Mouni, L. Adsorption Performance of Zeolite for the Removal of Congo Red Dye: Factorial Design Experiments, Kinetic, and Equilibrium Studies. *Separations* **2023**, *10*, 57. [[CrossRef](#)]
45. Emami, M.R.S.; Amiri, M.K.; Zaferani, S.P.G. Removal Efficiency Optimization of Pb²⁺ in a Nanofiltration Process by MLP-ANN and RSM. *Korean J. Chem. Eng.* **2021**, *38*, 316–325. [[CrossRef](#)]
46. Biradar, V.R.; Charde, M.S.; Chakole, R.D. QBD Approach Based Development of Validated Analytical Method for Estimation of Clarithromycin by RP-HPLC. *J. Adv. Sci. Res.* **2023**, *14*, 15–24. [[CrossRef](#)]
47. Jawad, A.H.; Abdulhameed, A.S.; Hanafiah, M.A.K.M.; AlOthman, Z.A.; Khan, M.R.; Surip, S.N. Numerical Desirability Function for Adsorption of Methylene Blue Dye by Sulfonated Pomegranate Peel Biochar: Modeling, Kinetic, Isotherm, Thermodynamic, and Mechanism Study. *Korean J. Chem. Eng.* **2021**, *38*, 1499–1509. [[CrossRef](#)]
48. Al-Ghouti, M.A.; Da'ana, D.A. Guidelines for the Use and Interpretation of Adsorption Isotherm Models: A Review. *J. Hazard. Mater.* **2020**, *393*, 122383. [[CrossRef](#)] [[PubMed](#)]
49. Candido, I.C.M.; Soares, J.M.D.; de Araujo Barros Barbosa, J.; de Oliveira, H.P. Adsorption and Identification of Traces of Dyes in Aqueous Solutions Using Chemically Modified Eggshell Membranes. *Bioresour. Technol. Rep.* **2019**, *7*, 100267. [[CrossRef](#)]
50. Mokhtar, N.; Aziz, E.A.; Aris, A.; Ishak, W.F.W.; Mohd Ali, N.S. Biosorption of Azo-Dye Using Marine Macro-Alga of *Euchema spinosum*. *J. Environ. Chem. Eng.* **2017**, *5*, 5721–5731. [[CrossRef](#)]
51. Poothachaya, P.; Puangsap, W.; Bunchalee, P.; Plangklang, P.; Reungsang, A.; Yuangsoi, B.; Cherdthong, A.; Tengjaroenkul, B.; Wongtangtharn, S. Investigation of Nutritional Profile, Protein Solubility and in Vitro Digestibility of Various Algae Species as an Alternative Protein Source for Poultry Feed. *Algal Res.* **2023**, *72*, 103147. [[CrossRef](#)]
52. Elgarahy, A.M.; Elwakeel, K.Z.; Mohammad, S.H.; Elshoubaky, G.A. A Critical Review of Biosorption of Dyes, Heavy Metals and Metalloids from Wastewater as an Efficient and Green Process. *Clean. Eng. Technol.* **2021**, *4*, 100209. [[CrossRef](#)]
53. Arumugam, N.; Chelliapan, S.; Kamyab, H.; Thirugnana, S.; Othman, N.; Nasri, N.S. Treatment of Wastewater Using Seaweed: A Review. *Int. J. Environ. Res. Public Health* **2018**, *15*, 2851. [[CrossRef](#)] [[PubMed](#)]
54. Bayramoglu, G.; Burcu Angi, S.; Acikgoz-Erkaya, I.; Yakup Arica, M. Preparation of Effective Green Sorbents Using *O. princeps* Alga Biomass with Different Composition of Amine Groups: Comparison to Adsorption Performances for Removal of a Model Acid Dye. *J. Mol. Liq.* **2022**, *347*, 118375. [[CrossRef](#)]
55. Yu, L.; Bi, J.; Song, Y.; Wang, M. Isotherm, Thermodynamics, and Kinetics of Methyl Orange Adsorption onto Magnetic Resin of Chitosan Microspheres. *Int. J. Mol. Sci.* **2022**, *23*, 13839. [[CrossRef](#)] [[PubMed](#)]
56. Hady, A.K.; Owda, M.E.; Abouzeid, R.E.; Shehata, H.A.; Elzaref, A.S.; Elfeky, A.S. Harnessing the Potential of Modified Cellulosic Pumpkin Seed Hulls as Affordable Biosorbents for Cationic Dye Removal from Aqueous Solutions: Adsorption Kinetics and Isotherm Studies. *Biomass Convers. Biorefin.* **2023**. [[CrossRef](#)]
57. Yönten, V.; Sanyürek, N.K.; Kivanç, M.R. A Thermodynamic and Kinetic Approach to Adsorption of Methyl Orange from Aqueous Solution Using a Low Cost Activated Carbon Prepared from *Vitis vinifera* L. *Surf. Interfaces* **2020**, *20*, 100529. [[CrossRef](#)]
58. Carolin, C.F.; Kumar, P.S.; Joshiba, G.J. Sustainable Approach to Decolourize Methyl Orange Dye from Aqueous Solution Using Novel Bacterial Strain and Its Metabolites Characterization. *Clean Technol. Environ. Policy* **2021**, *23*, 173–181. [[CrossRef](#)]
59. Murali, V.; Ong, S.A.; Ho, L.N.; Wong, Y.S. Evaluation of Integrated Anaerobic-Aerobic Biofilm Reactor for Degradation of Azo Dye Methyl Orange. *Bioresour. Technol.* **2013**, *143*, 104–111. [[CrossRef](#)]
60. Zhong, W.; Jiang, T.; Dang, Y.; He, J.; Chen, S.Y.; Kuo, C.H.; Kriz, D.; Meng, Y.; Meguerdichian, A.G.; Suib, S.L. Mechanism Studies on Methyl Orange Dye Degradation by Perovskite-Type LaNiO₃- Δ under Dark Ambient Conditions. *Appl. Catal. A Gen.* **2018**, *549*, 302–309. [[CrossRef](#)]

Disclaimer/Publisher's Note: The statements, opinions and data contained in all publications are solely those of the individual author(s) and contributor(s) and not of MDPI and/or the editor(s). MDPI and/or the editor(s) disclaim responsibility for any injury to people or property resulting from any ideas, methods, instructions or products referred to in the content.